Novel waveform for magnetron radar

N. Levanon, E. Ben-Yaacov †, D. Quartler**

**Tel-Aviv University, Israel, nadav@eng.tau.ac.il, †Elbit Systems-Elisra, Israel, Erez.Ben-Yaacov@elbitsystems.com*

Keywords: Radar, waveform, magnetron, PRI-coding.

Abstract

Magnetron does not lend itself to pulse-compression. To achieve narrow range resolution it must transmit short pulses. For given peak-power, antenna-gain and rotation-rate, increasing energy-on-target can be achieved by increasing the pulse repetition frequency (PRF), which is ordinarily limited by the specified unambiguous range. The proposed pulse-train waveform unties the two. Transmitting the first or second out of each pair of pulses of a uniform pulse-train, according to a periodic code, can extend the unambiguous range considerably beyond what the original PRF determines. In the receiver the envelope-detected return-pulses are correlated with a corresponding mismatched bipolar pulse-train. In addition to extending the unambiguous range, this detection concept performs Marcum's alternative integration scheme of "(signal + noise) − noise", exploiting its benefits. Successful coastal trials with modified civil marine magnetron radar are described.

1 Introduction

Magnetron lost its main roll in radar when pulse-compression and moving target indication (MTI) became critical features. Pulse-compression provides the resolution of a short pulse with the energy of a long pulse, through intra-pulse frequency or phase modulation, of which the magnetron is incapable. MTI or Doppler-processing requires phase stability from pulse to pulse, while in magnetron the starting phase of each pulse is random from pulse to pulse. Yet, magnetron's simplicity, high power and low-cost, keeps it the transmitter of choice for use in civil marine radar [1], where Doppler processing is not required. Without pulse-compression, the only way to get narrow range resolution is short pulse. Indeed, for short-range setting, a typical magnetron pulse-width is 80nsec, providing range resolution of 12m. The corresponding typical PRF is 3kHz, providing unambiguous range of 50km. For long-range setting the PRF is reduced to 600Hz (unambiguous range of 250km). To maintain the average power, the pulse-width is increased to about 1μs. To further increase the energy on target the antenna rotation rate is slowed down at the long distance setting. Long pulse comes with two penalties: Poor range resolution and larger clutter illumination area. It would have been beneficial if short pulses could be transmitted also at the long-range settings of the radar, with average power restored by using high-PRF. The waveform we suggest does exactly that, but without reducing the unambiguous range. The paper describes the suggested transmitted and reference waveforms, the resulted theoretical range response, and the actual performances obtained from coastal trials, with modified commercial magnetron radar.

2 Waveforms

The waveform is a train of short pulses whose pulse repetition interval (PRI) is periodically coded [2]. The code is based on a binary sequence that exhibits ideal periodic autocorrelation, or ideal periodic cross-correlation with a slightly different reference sequence. Two codes were used in the field trials. One was based on Barker 4, which is the only known binary sequence with ideal periodic autocorrelation. The second was based on Ipatov 5 code [3]. Binary codes use two values {+1, −1}, but a magnetron cannot be polarity modulated; it can only be on-off keyed. So the Barker 4 is Manchester coded: +1 is converted to {0, 1} and −1 to {1, 0}. "1" implies transmitted pulse and "0" implies omitted pulse.

In the receiver, the envelope detected pulse train is correlated not with a matched sequence of "1" and "0"s; but with a reference sequence constructed from "+1" and "−1", respectively. The reference sequence is implemented numerically and can take any value. Rows 2 and 3 of Table 1 list one period (8 PRIs in a period, $\mathrm{PRI} = T_r$) of the transmitted pulses and the reference sequence of Barker 4 based signal. Fig. 1 displays five transmitted code periods (top) and two reference periods (bottom). Omitted pulses in the transmitted train appear as negative pulses in the reference sequence. This mismatched filter produces cross-correlation (Fig. 2) that differs from ideal periodic response only by two negative sidelobes (SL) at $\pm T_r$ around the periodic mainlobe. The depth of the negative SL is half the height of the mainlobe. The response periodicity is 8 PRIs, implying extension of the unambiguous range by a factor of 8. In reality the periodic transmission continues indefinitely and the length of the reference is set according to the time-on-target (TOT) provided by the rotating antenna.

3 Modified reference

The main drawback of the delay response in the top subplot of Fig. 3 is the strong negative sidelobe at a delay $\tau = T_r$. It implies that the strong direct reception of the transmitted pulse, followed by strong returns from near-clutter, which appear at and immediately after $\tau = 0$, will also create a

corresponding deep null ("hollow") at and immediately following $\tau = T_r$. The depth of the "hollow" is half the height of the direct reception and the near-clutter. True targets near that delay are likely to be concealed in the "hollow". There is therefore a motivation to push that "hollow" farther away and make it shallower.

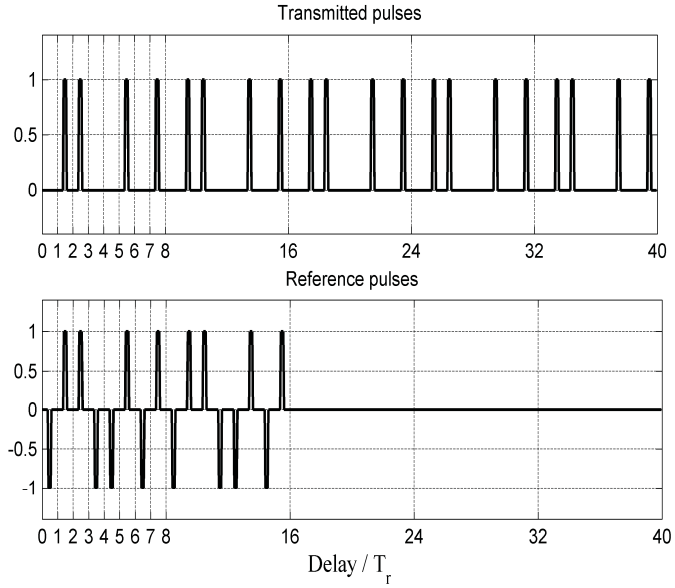

Fig. 1. Transmitted and reference pulse trains based on Manchester-coded Barker 4 sequence.

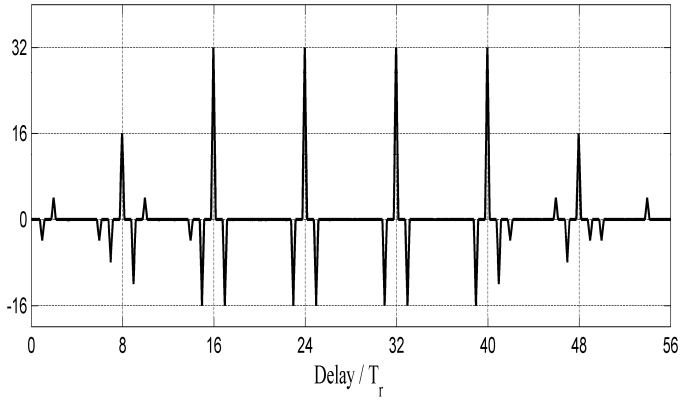

Fig. 2. Cross-correlation of the transmitted and reference pulse trains in Fig. 1.

Pulse#	1	2	3	4	5	6	7	8
Trans.	0	1	1	0	1	0	1	0
Ref. 1	–1	1	1	–1	1	–1	1	–1
Ref. 2	–0.5	1.5	0.5	–0.5	0.5	–0.5	0.5	–1.5
Ref. 3	–0.75	1.25	0.75	–0.75	0.75	–0.75	0.75	–1.25
Ref.NC	0	1	1	0	1	0	1	0

Table 1: Transmitted and reference pulses based on Barker 4.

Ref. 2 (4th row of Table 1) achieves that. Under ideal conditions, in which all the transmitted pulses have identical amplitude; the response attained with Ref. 2 will be optimal. It is shown in the middle subplot of Fig. 3. In practice, the transmitted pulses are not identical. For example, when the PRI is reduced considerably below its original value, the magnetron pulses tend to change amplitude in some relation to the pause they follow. Furthermore, the transmitted and received pulses are modulated by the rotating antenna beam. When the transmitted pulses are not identical the response obtained with the three references listed in Table 1 may look like the plots in Fig. 4. The positive sidelobe at delay = PRI (marked by the arrow) is the most bothersome. It will cause the direct reception and near-clutter to reappear as *positive* sidelobes around that delay. Even when these positive sidelobes are attenuated by 50 or 60dB, they still are of similar intensity to expected true targets at that delay. The variable amplitudes issue prompted the use of Ref. 3 (see Tables 1). The ideal response of Ref. 3 exhibits two shallow negative hollows at PRI and 2*PRI (see Fig. 3, lower subplot). Those sidelobes are expected to remain negative (Fig. 4, lower subplot) despite intensity fluctuations of the transmitted pulses. Refs. 2 and 3 are obtained from Ref. 1 as follows:

$$R_2(n) = R_1(n) + 0.5R_1(n+1). \quad (1)$$

$$R_3(n) = R_1(n) + 0.25R_1(n+1). \quad (2)$$

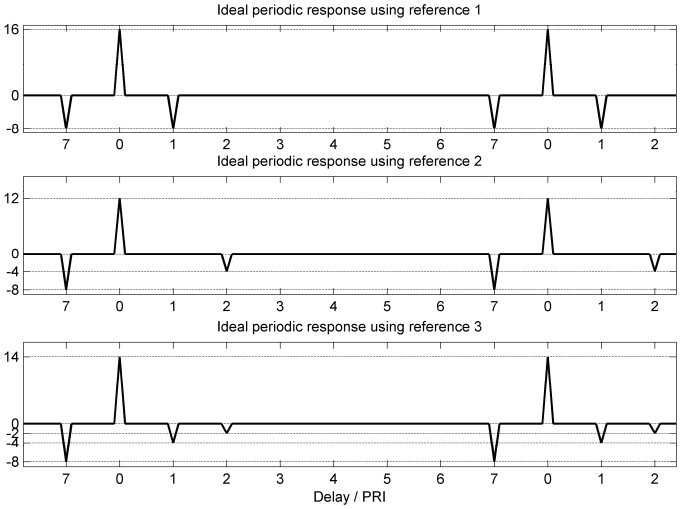

Fig. 3. Three responses obtained with the three references listed in Table 1 (Identical transmitted pulses).

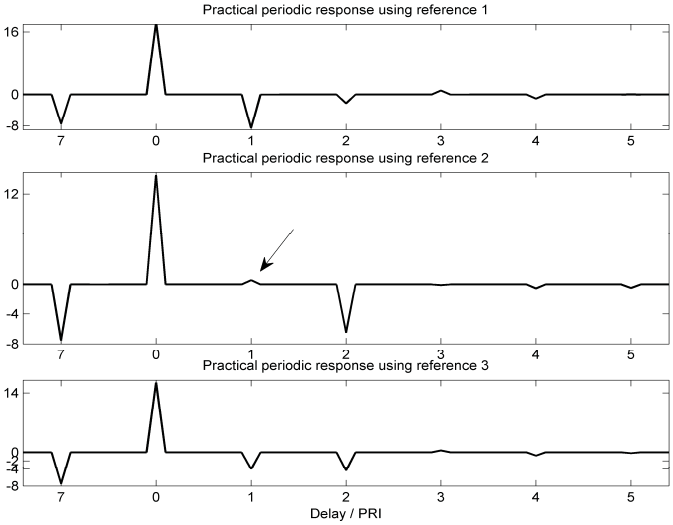

Fig. 4. Three responses obtained with the three references in Table 1 (Fluctuating transmitted pulses).

Pulse #	1	2	3	4	5	6	7	8	9	10
Trans.	1	0	1	0	1	0	0	1	1	0
Ref. 1	1	−1	1	−1	1	−1	−2	2	1	−1
Ref. 2	0.5	−0.5	0.5	−0.5	0.5	−2	−1	2.5	0.5	−0.5
Ref. 3	0.75	−0.75	0.75	−0.75	0.75	−1.75	−1.25	2.25	0.75	−0.75
Ref. NC	1	0	1	0	1	0	0	1	1	0

Table 2: Transmitted and reference pulses based on Ipatov 5.

4 Detection properties

J. I. Marcum, in his seminal 1947 research memorandum [4] suggested a different scheme for noncoherent integration "*... in which a pulse known to be only noise is subtracted from each possible signal plus noise pulse. N of these composite pulses are then integrated. With no signal, the average value of any number of such composite pulses is nearly zero ...*" In our integration approach this detection scheme is built-in. Note in Fig. 1 that each omitted transmitted pulse (hence received noise) is multiplied by a negative reference pulse (hence the noise subtraction).

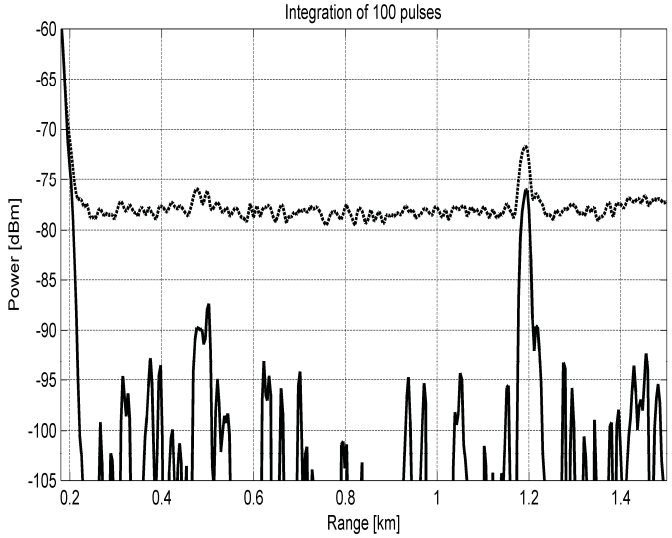

Fig. 5. Detector output using conventional noncoherent integration (dash) and Ipatov processing (solid).

The example in Fig. 5 shows detector outputs from a calm sea scene with a small boat at 1.2km. Ipatov-based coding [3] was used (Table 2). The reference for the conventional noncoherent integration of 100 pulses was 20 sequences of Ref. NC, and yielded the dash line. The reference for the PRI-coded processing was 20 sequences of Ref. 1, and yielded the solid line.

Since our Barker/Ipatov processing implements Marcum's "(signal + noise) − noise" integration scheme, we expect the output, when detecting noise, to be centred near zero. Indeed this is confirmed by the solid line plot in Fig. 5 (only positive values were used before converting to logarithmic scale). The mean of the conventional noncoherent integration of noise (around −78dBm) hints that setting adaptive threshold for constant false alarm ratio (CFAR) will require estimation of two parameters (mean and variance), while for Barker/Ipatov processing only the variance needs to be estimated.

5 Field trial results

The field trials were conducted with Furuno 1623, a low-cost, magnetron, civil marine radar. The radar was altered slightly to provide control of pulse triggering and to extract the IF output. The radar operates at X-band (9.41 GHz). It has a 15" antenna, providing 6.2 degree horizontal beam-width. The peak pulse-power is 2.2kW. We mainly used the short pulses (0.08μs). At that pulse-width the antenna rotation rate is 41 rpm. Thus a point target is illuminated for 25ms every 1.46s. At a nominal PRF of 6250Hz, the 8 pulse positions in a Barker-coded period occupy 1.28ms, namely, the target illumination contains approximately 19 Barker-coded periods or 72 transmitted pulses. This is therefore the length of the reference sequence. Hamming-weight amplitude-multiplies the reference sequence. 240 pulses are integrated when the highest (20kHz) PRF is used. The main purposes of the field trial were: (a) to test the extension of the unambiguous range by the proposed coding (Barker and Ipatov); (b) to demonstrate the improved resolution of using short pulses. To be able to see targets beyond the un-coded unambiguous range (= C/PRF/2) we needed distant large ships. The required scene can be found near the port of Ashdod. The radar was mounted on a tripod placed on a small dune in the southern most beach of the city of Ashdod (Fig. 6). The port of Ashdod and the area of waiting ships were to the north and north-west. We also detected ships waiting to unload fuel for the power station in Ashkelon at the south.

Fig. 6. The radar set up.

We raised the PRF from 3kHz to values between 6 and 20kHz (half the pulses are not transmitted). The results shown in this paper were taken with PW = 80nsec and PRF = 12.5kHz. The PRF-coded transmission was processed using Barker/Ipatov references (using Ref. 3 in tables 1 and 2), and simultaneously using matched references (Ref. NC in tables 1 and 2). There was also (non-simultaneously) a comparison with conventional uncoded transmission, with PW of 800nsec and uniform PRF of 625Hz. Without Barker/Ipatov processing, PRF = 12.5kHz implies unambiguous range of 12km. With Barker/Ipatov processing, the corresponding unambiguous ranges become 96km (Barker) and 120km (Ipatov).

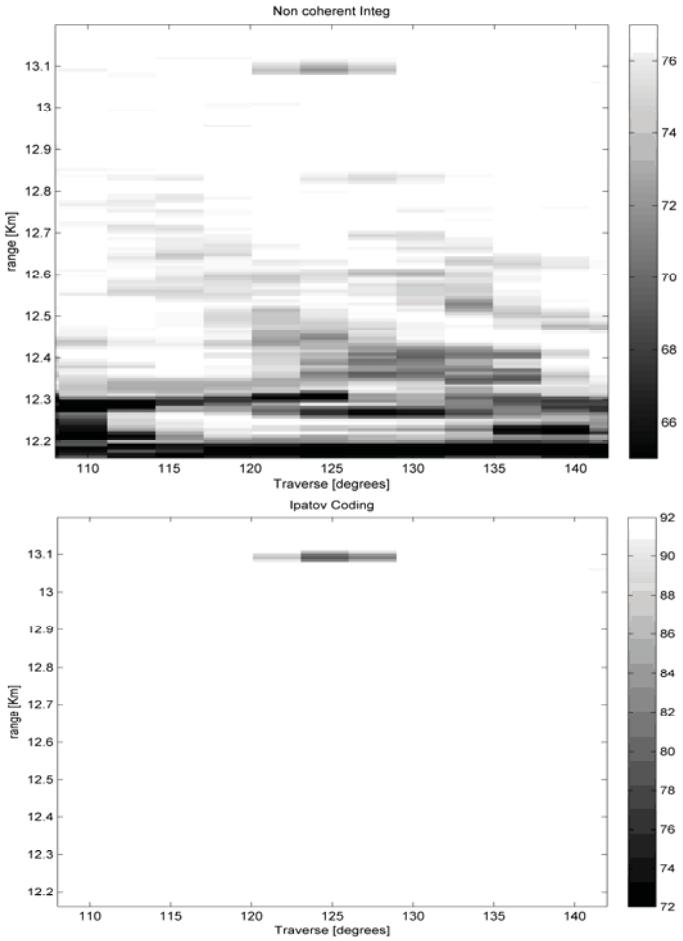

Fig. 7 A ship at 13.1km, PW= 80ns, PRF=12.5kHz. Top: Noncoherent integration. Bottom: Ipatov processing.

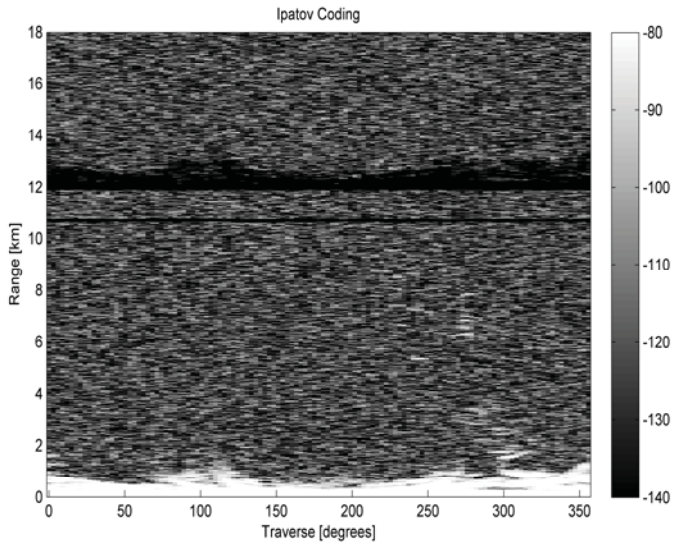

Fig. 8. The "hollow" (or "blind range") at 12km. Ipatov processing. PW=80ns, PRF=12.5kHz. (The additional narrow "hollow" at 10.8km resulted from a hardware flaw.)

Both parts of Fig. 7 were obtained from the same single antenna sweep, using Ipatov-coded transmission. They provide comparison between noncoherent integration (top part) and Ipatov processed integration (bottom). The detected target is a ship at 13.1km facing Ashkelon. The graybar is in negative dB. With PRF=12.5kHz the unambiguous range is 12km. Indeed in the top part of Fig. 7 the near-clutter replicates at and beyond 12km, making it difficult not to confuse the ship with replicated near-clutter. Due to Ipatov processing, in the bottom part of Fig. 7 the ship is in the clear. Where the near clutter was seen before there is now a "hollow". The "hollow" at 12km is made visible in Fig. 8 by extending the dynamic range and reversing the sign of the graybar. This blind-range difficulty can be mitigated by switching PRFs between consecutive antenna revolutions and performing "one out of two" binary integration on two revolutions.

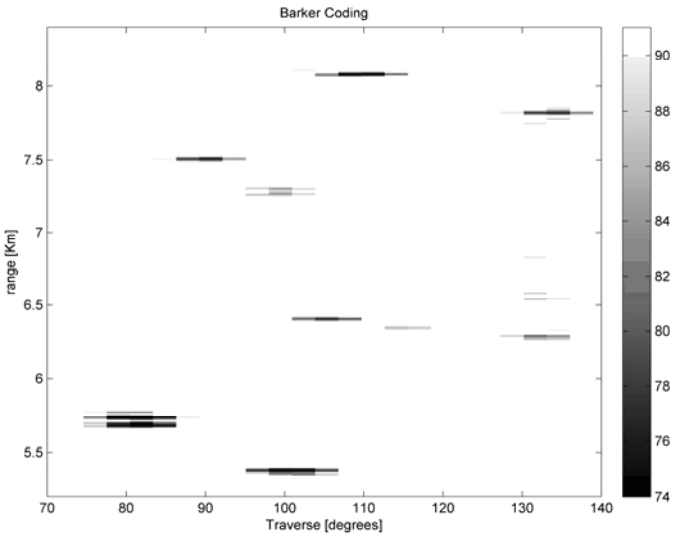

Fig. 9. Ships facing Ashdod. Barker processing. PW= 80ns, PRF=12.5kHz.

Fig. 9 demonstrates the improved range resolution obtained with the narrow pulse (80nsec). It displays a cluster of ships facing the port of Ashdod. The transmitted sequence was Barker-coded. Fig. 9 displays the result of processing a single antenna sweep, using Ref. 3 in tables 1. The same returns were also processed using Ref. NC in Table 1. Up to the unambiguous range of 12km they yielded very similar detection results.

The pixel range width is 7.5m, smaller than the range resolution (12m) of an 80ns pulse. The traverse pixel width is 3^0, half the antenna beam-width. 3^0 convert to about 300m at a range of 5.7km. Observing the two nearest targets, Fig. 9 suggests that the ship at 5.7 km is aligned approximately along the radial direction, while the ship at 5.4km is aligned approximately cross-range. The zoom in Fig. 10 details the range profile of the ship at 5.7km. It suggests the ship's total range span of 150m, divided into 3 or 4 along-range scattering zones. This profile is supported by the photograph in Fig. 12. In order to demonstrate how much the range resolution was improved by the short pulse, Fig. 11 shows the same ship as in Fig. 10 (taken several hours apart) with the radar in its original mode (PW = 800ns, PRF = 625Hz, rotation speed = 24rpm). Note that the traverse scale is randomly offset from one run to another, and that the traverse pixel width in this mode is about 5^0. With range resolution of 120m and pixel range width of 75m, little or no information on aspect and radial dimensions can be deduced.

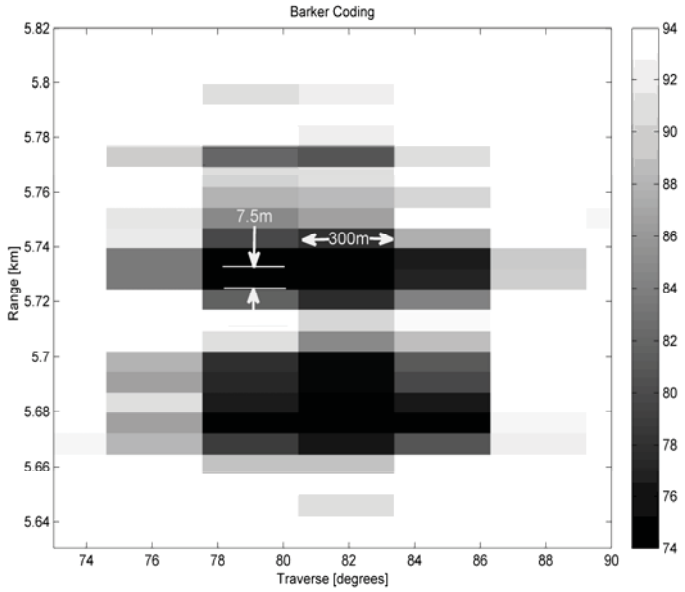

Fig. 10. Zoom on the ship at 5.7km. PW= 80ns.

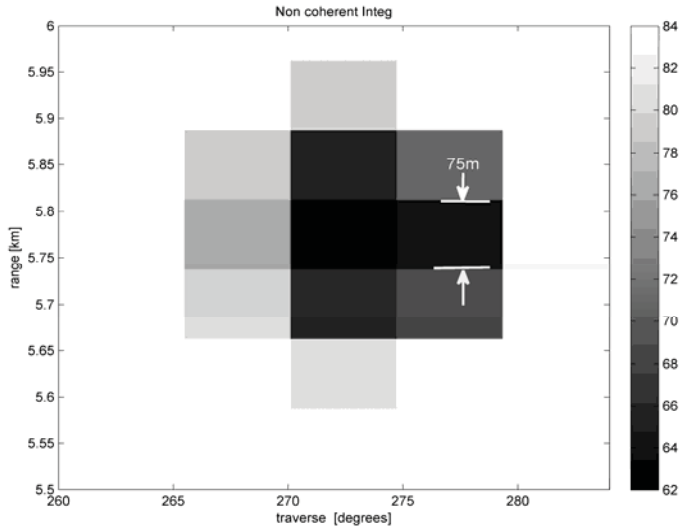

Fig. 11. Zoom on the ship at 5.7km. Noncoherent integration, PW = 800ns, PRF = 625Hz.

Fig. 12. The ship whose radar profiles appear in Figs.10-11.

6 Interference mitigation

Taking over all the receiver operations after the IF amplifier meant losing some built-in features of the original radar. We did not try to reproduce all the features and controls in order to create a fully operational product. However one issue needed attention and that was interference from marine radar on other ships. The quick ad-hoc fix to this kind of interference was to repeatedly arrange the sampled detection in a numerical array in which each row contained the detected samples from one coded period (e.g., from 10 nominal PRIs, in the Ipatov case), and the number of rows was equal to the number of code sequences to be integrated later (e.g., 20 rows, when integrating returns from 100 transmitted pulses). Thus each column represents a range bin. On each column we removed any detection which is 10dB over the 60^{th} percentile of all the elements in that column, and replaced it with its neighbours. Once those outliers were removed, the integration (= correlation) was performed.

7 Mitigating blind ranges

The main penalties of the demonstrated approach are blind ranges ("hollow" in the response), at delays equal to the PRI (Fig. 8) and its multiples. The hollow width equals the width of the *strong* near-clutter. In our experiment, with the radar on shore, that width was approximately 300m. In case of radar at sea the range span of the strong near-clutter is expected to be narrower, resulting reduced chance of concealing targets. The blind range difficulty can be mitigated by switching, once per antenna revolution, between two slightly different PRIs.

Combining PRI switching between consecutive antenna scans, with detection decisions based on binary integration of two antenna scans, and a binary integration rule of "at least one-out-of-two", is likely to reveal all detectable targets. The small chance of having a target in the blind range, and the high effectiveness of binary integration, promise this to be a good fix. In stationary (coastal) radar, the binary integration can be extended over more antenna scans. Fig. 13 demonstrates the outcome of 2-out-of-10-scans binary integration, following along-range CFAR. The cluster of ships facing the port of Ashdod is centred around (5, 5) km. The ship facing Ashkelon is at (-13, 2) km. The azimuth spread is caused by the wide antenna's 3dB beamwidth (6.2^0) and the azimuth pixel width (3^0). In ship-borne radar the number of integrated scans will be limited by the number of antenna scans during which the radar can be considered stationary.

8 Summary and discussion

Our experimental results show the feasibility of extending the unambiguous range of magnetron pulse radar. On transmit; half of the pulses are eliminated according to a periodic code. On receive; the pulses are envelope-detected and then cross-correlated with numerically implemented reference pulses that use two polarities and variable amplitudes. This concept allows operating the radar in a "short pulse, short PRI" mode even at long range settings.

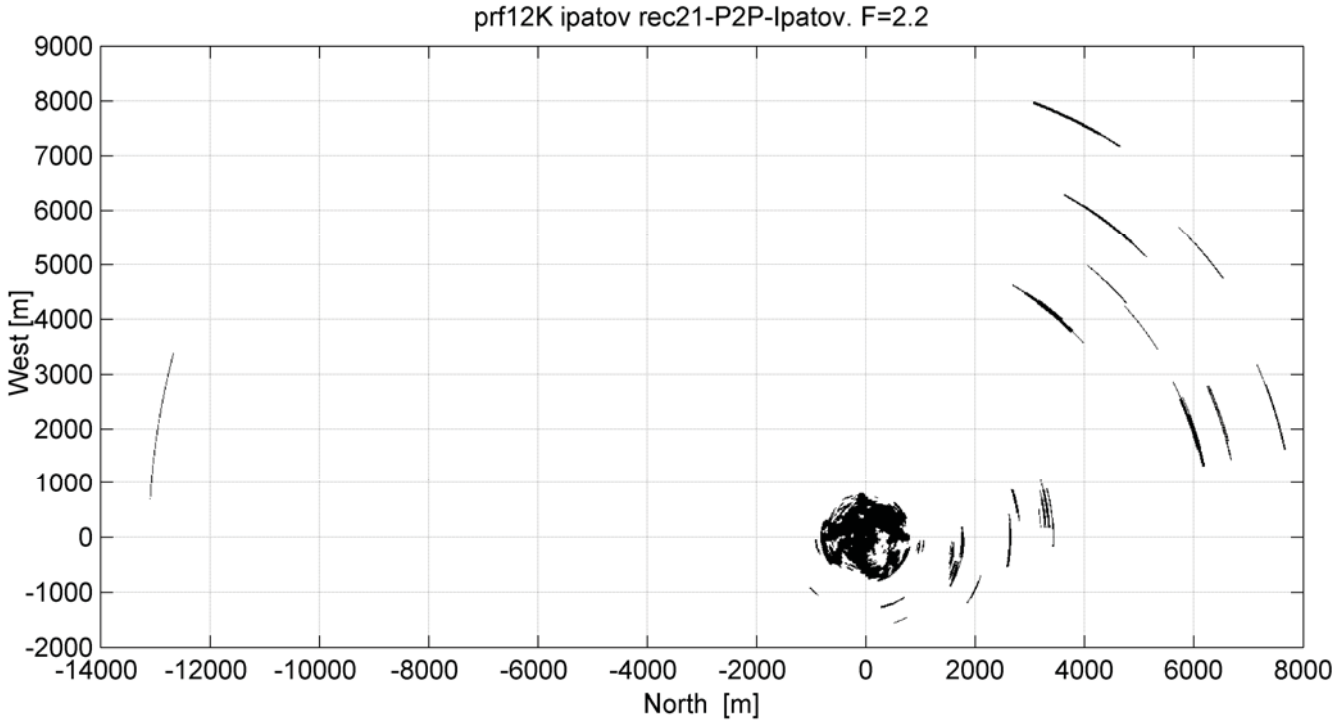

Fig. 13. Radar scene after Ipatov integration, along-range CFAR, and 2-out-of-10-scans binary integration. PRF = 12.5kHz.

The "short pulse, short PRI" mode maintains the average transmitted power, improves the range resolution and reduces clutter illumination. Being able to use short pulses is especially important in magnetron radar, where there is no option to perform pulse-compression. The experiment was performed using modified low-cost 2.2kW magnetron radar (Furuno 1623). 80ns pulses were transmitted at PRFs as high as 20kHz. Another advantage of short pulses, reduced clutter illumination area, could not be demonstrated because of calm sea during our field trials.

The special form of the reference signal implements Marcum's alternative noncoherent detection scheme "(signal plus noise) minus noise". The small SNR loss (~1dB), predicted by Marcum and by our own simulations, was indeed observed in the field trial. Up to the original unambiguous range, both detection schemes yielded similar detection probabilities. Note also that the zero average output, when our scheme detects noise only, is helpful in threshold setting.

References

[1] J. N. Briggs. *Target Detection by Marine Radar*. IEE 2004.

[2] N. Levanon. "New waveform design for magnetron-based marine radar", *IET RSN,* 2009, **3**, (5), pp.530-540.

[3] N. Levanon, E. Mozeson. *Radar Signals*, Sec. 6.5, Wiley, Hoboken, NJ, 2004.

[4] J. I. Marcum. *A statistical theory of target detection by pulsed radar*, RAND Corp. Res. Mem. RM-754, 1 Dec. 1947. (Reprinted in the *IRE Trans. Inf. Theory*, Vol. **6**, No. 2, pp. 59-267, 1960)